

# Peculiar spectral statistics of ensembles of trees and star-like graphs

V. Kovaleva<sup>1</sup>, Yu. Maximov<sup>1,2</sup>, S. Nechaev<sup>3,4</sup>, and O. Valba<sup>5,6</sup>

<sup>1</sup> Center of Energy Systems, Skolkovo Institute of Science and Technology, Russia

<sup>2</sup> Center for Nonlinear Studies and Theoretical Division T-4,

Los Alamos National Laboratory, Los Alamos, NM 87545, USA

<sup>3</sup> CNRS/Independent University of Moscow, Poncelet Laboratory, Moscow, Russia

<sup>4</sup> P.N. Lebedev Physical Institute RAS, Moscow, Russia

<sup>5</sup> Department of Applied Mathematics, National Research University Higher School of Economics

<sup>6</sup> N.N. Semenov Institute of Chemical Physics of the Russian Academy of Sciences

In this paper we investigate the eigenvalue statistics of exponentially weighted ensembles of full binary trees and  $p$ -branching star graphs. We show that spectral densities of corresponding adjacency matrices demonstrate peculiar ultrametric structure inherent to sparse systems. In particular, the tails of the distribution for binary trees share the “Lifshitz singularity” emerging in the one-dimensional localization, while the spectral statistics of  $p$ -branching star-like graphs is less universal, being strongly dependent on  $p$ . The spectra of graphs’ adjacency matrices can be interpreted as sets of resonance frequencies, typical for ensembles of fully branched tree-like and star-like macromolecules, known as dendrimers.

## I. INTRODUCTION

One can gain the information about topological and statistical properties of polymers in solutions by measuring their relaxation spectra [1]. A rough model of an individual polymer molecule of any topology is a set of monomers (atoms) connected by elastic strings. If deformations of strings are small, the response of the molecule on external excitation is harmonic according to the Hooke’s law. The relaxation modes are basically determined by the so-called Laplacian matrix of the molecule.

Consider the polymer network as a graph or a collection of graphs, see Fig. 1a. Enumerate the monomers of the  $N$ -atomic macromolecule by the index  $i = 1 \dots N$ . The adjacency matrix  $A = \{a_{ij}\}$  describing the topology (connectivity) of a polymer molecule is symmetric ( $a_{ij} = a_{ji}$ ). Its matrix elements  $a_{ij}$  take binary values, 0 and 1, such that the diagonal elements vanish, i.e.  $a_{ii} = 0$ , and for off-diagonal elements,  $i \neq j$ , one has  $a_{ij} = 1$ , if the monomers  $i$  and  $j$  are connected, and  $a_{ij} = 0$  otherwise. The Laplacian matrix  $L = \{b_{ij}\}$  is by definition as follows:  $b_{ij} = -a_{ij}$  for  $i \neq j$ , and  $b_{ii} = \sum_{j=1}^N a_{ij}$ , as shown in Fig. 1b. The eigenvalues  $\lambda_n$  ( $n = 1, \dots, N$ ) of the symmetric matrix  $L$  are real.

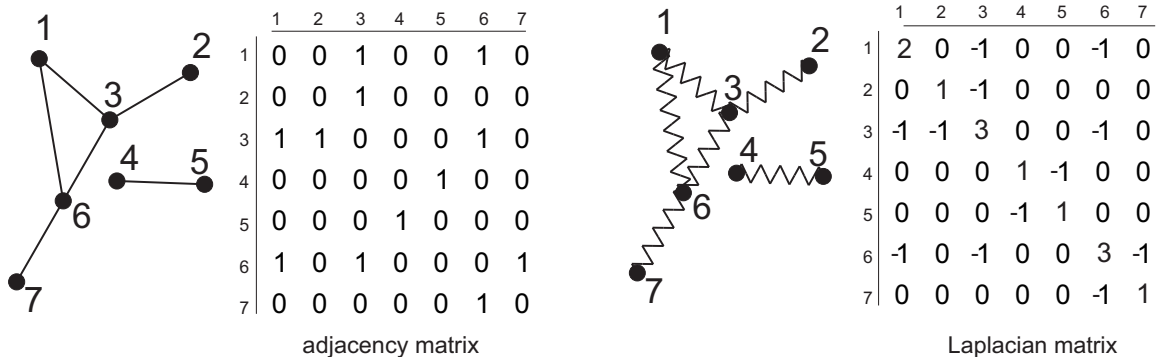


Figure 1: (a) Sample of a topological graph (collection of subgraphs) and its adjacency matrix; (b) Elastic network corresponding to (a) and its Laplacian matrix.

In physical literature the adjacency matrix spectrum is interpreted as the set of resonance frequencies, while the Laplacian spectrum defines the relaxation of the system. Thus, measuring the response of the diluted solution of noninteracting polymer molecules on external excitations with continuously changing wavelength, we expect to see the signature of eigenmodes in the spectral density as peaks at some specific frequencies. Some other applications of adjacency and Laplacian matrices in graph theory and optimization are thoroughly described in [2] and [3].

Previously, in [4] the eigenvalue density in ensembles of large sparse random adjacency matrices was investigated. It was demonstrated that the fraction of linear subgraphs at the percolation threshold is about 95% of all finite subgraphs, and the distribution of linear subgraphs (chains) is purely exponential. Analyzing in detail the spectral density of linear chain ensembles, the authors claim in [4] its ultrametric nature and showed that near the edge of the spectrum,  $\lambda_{max}$ , the tails of the spectral density,  $\rho(\lambda)$  exhibit a Lifshitz singularity,  $\rho(\lambda) \sim e^{-c/\sqrt{\lambda_{max}-\lambda}}$ , typical for the one-dimensional Anderson localization. Also the attention was paid to a connection of the spectral density to the modular geometry and, in particular, to the Dedekind  $\eta$ -function. In [4] it was conjectured that ultrametricity emerges in any rare-event statistics and is inherit to generic complex sparse systems.

The rare-event statistics has many manifestations in physics [5] and biophysics [6]. For example, the contact maps of individual DNA molecules in cell nuclei are sparse. Thus, experimenting with physical properties of highly diluted solutions of biologically active substances, one should pay attention to a very peculiar structure of background noise originating from the rare-event statistics of dissolved clusters. In this case, the peculiar shape of noise spectrum can be misinterpreted or at least can make the data incomprehensible [7–9]. In order to make conclusions about any biological activity of regarded chemical substance, the signal from background noise should be clearly identified. From this point of view, the work [10] seems very interesting, since it represents an exceptional example of careful attention to ultrametric-like distributions in biological and clinical data.

In the current work we investigate in detail the spectral statistics (eigenvalue density of the adjacency matrices) of branched polymer ensembles: (i) complete three-branching trees, and (ii)  $p$ -branching star-like graphs. These structures represent special cases of polymers of peculiar topology, known as *dendrimers* [11]. Computing the eigenvalues (resonances) of the adjacency matrix, and the degeneracy of these resonances in the polymer ensemble, we provide the complete information about the excitation statistics, analyze the tails of corresponding distributions and discuss the origin of clearly seen *ultrametricity* [12, 13]. We obtain the results for adjacency matrices (but not for the Laplacian ones) to make our conclusions comparable with former research dealt with linear chain ensembles. We conjecture that one can witness the corresponding relaxation spectral statistics in real experiments and/or in relevant molecular dynamic simulations.

To make the content of the paper as self-consistent as possible, we remind briefly the notion of ultrametricity. A metric space is a set of elements equipped by pairwise distances,  $d(x, y)$  between elements  $x$  and  $y$ . The metric  $d(x, y)$  meets three requirements: i) non-negativity,  $d(x, y) > 0$  for  $x \neq y$ , and  $d(x, y) = 0$  for  $x = y$ , ii) symmetry,  $d(x, y) = d(y, x)$ , and iii) the triangle inequality,  $d(x, z) \leq d(x, y) + d(y, z)$ . The concept of ultrametricity is related to a special class of metrics, obeying the *strong triangular inequality*,  $d(x, z) \leq \max\{d(x, y), d(y, z)\}$ .

The description of ultrametric systems in physical terms deals with the concept of hierarchical organization of energy landscapes [12, 13]. A complex system is assumed to have a large number of metastable states corresponding to local minima in the potential energy landscape. With respect to the transition rates, the minima are suggested to be clustered in hierarchically nested basins, i.e. larger basins consist of smaller basins, each of those consists of even smaller ones, *etc.* The basins of local energy minima are separated by a hierarchically arranged set of barriers: large basins are separated by high barriers, and smaller basins within each larger one are separated by lower barriers.

Since the transitions between the basins are determined by the passages over the highest barriers separating them, the transitions between any two local minima obey the strong triangle inequality. The ultrametric organization of spectral densities obtained in our work should be understood exactly in that sense, if we identify the degeneracy of the eigenvalue with the height of the barrier separating some points on the spectral axis. Ultrametric geometry fixes taxonomic (i.e. hierarchical) tree-like relationships between elements and, speaking figuratively, is closer to Lobachevsky geometry, rather than to the Euclidean one.

The selection of binary trees and stars for our study is not occasional. We are interested in the question whether the hierarchical structure of spectral density emerges in polymer ensembles beyond the linear statistics. Moreover, ensembles of full binary trees and stars allow for complete analytic treatment, which makes them the first candidates beyond the rare-event statistics emerging in linear ensembles. Varying the branching number of star-like graphs, we can interpolate between linear chains and branching structures, attempting to understand the influence of non-linear topology on spectral statistics.

It is essential to emphasize that we investigate ensembles of non-interacting polymer molecules. This is ensured by the low density of polymers in the solution [14]. Understanding how the inter-molecular interactions change the spectral density of the polymer solution is a challenging problem which yet is beyond the scopes of our investigations, however definitely will be tackled later. Additional remarks should be made regarding the polymer size distribution in ensembles. It is crucial that we study *polydisperse* ensembles (i.e. ensemble of polymers of various sizes). Here we suppose the probability  $\mathbb{P}(N)$  to find an  $N$ -atomic chain, to be exponential,  $\mathbb{P}(N) \sim e^{-\mu N}$  ( $\mu > 0$  is some constant rate of joining monomers together in a course of a polymer assembling). The choice of the exponential distribution is

mainly motivated by the work [4] where such a distribution appeared naturally at the percolation threshold following from the random Bernoulli-type construction of long linear sequences. However, we can consider any other distribution and the selection of the exponential one is mainly the question of convenience: the comparison of new and old results in this case is much more straightforward.

## II. GRAPHS UNDER CONSIDERATION: FULL BINARY TREES AND STARS

In [4] the authors discussed some statistical properties of polydisperse ensembles of linear macromolecules and paid attention to two specific properties: i) the singularity of the enveloping curve of spectral density at the edge of the spectrum, known as the “Lifshitz tail”, and ii) the hierarchical organization of resonances in the bulk of the spectrum. It was shown in [4] that these properties are inherent to generic sparse ensembles and can be viewed as number-theoretic manifestations of the rare-event statistics. Whether they survive for ensembles of trees or stars is the question analyzed in present work.

Below we compute eigenvalues with corresponding multiplicities (degeneracies) of adjacency matrices of full binary trees and star-like graphs (dendrimers), schematically depicted in Figs. 2a,b. Then we perform averaging over ensembles of trees of particular topology and determine the spectral density.

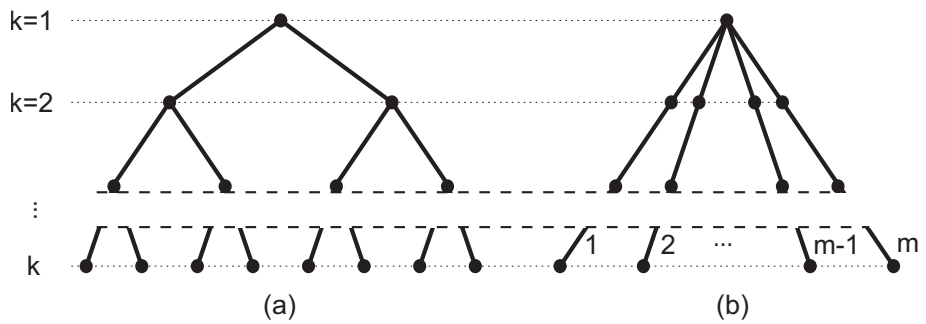


Figure 2: (a) Full binary tree; (b) a star-like graph with  $p$  branches of  $k$  nodes.

Let  $\mathcal{T}_k$  be a full binary tree of level  $k$  shown in the Fig. 2a. The shortest path from the root of  $\mathcal{T}_k$  to any leaf is  $k-1$ , and the tree has  $2^k - 1$  vertices in total. Let  $\mathbf{T}_k$  be the adjacency matrix of  $\mathcal{T}_k$ . The spectrum of an individual tree  $\mathbf{T}_k$  has exactly  $\mathcal{N}_k^{tree} = 2^k - 1$  eigenvalues, all real. Let  $\rho_k(\lambda)$  be the spectral density of  $\mathbf{T}_k$ ,

$$\rho_k(\lambda) : \mathbb{R} \rightarrow \mathbb{R},$$

where  $\lambda$  is an eigenvalue, and  $\rho_k(\lambda)$  is its frequency (degeneracy) defined as the quotient of its multiplicity  $M_k(\lambda)$  and the total number of eigenvalues  $\mathcal{N}_k^{tree}$ . We investigate the ensemble of such trees with the exponential distribution,

$$\mathbb{P}_\mu(k) = Ce^{-\mu k}, \quad \sum_{k=1}^{\infty} \mathbb{P}_\mu(k) = 1, \quad (1)$$

where  $C = e^\mu - 1$ , and  $\mu$  is a parameter. The spectral density,  $\rho(\lambda)$  of the ensemble is the quotient of multiplicity expectation and tree size expectation

$$\rho(\lambda) = \frac{\sum_{k=1}^{\infty} \mathbb{P}_\mu(k) M_k(\lambda)}{\sum_{k=1}^{\infty} \mathbb{P}_\mu(k) \mathcal{N}_k^{tree}}. \quad (2)$$

For a star graph depicted in the Fig. 2b we state the problem similarly. Let  $\mathcal{S}_{k,p}$  be a star graph constructed by gluing  $p$  linear graphs (chains) at one point, all extended up to the level  $k$ . The graph has  $p(k-1) + 1$  vertices in total, and its adjacency matrix is  $\mathbf{S}_{k,p}$  with the total number of eigenvalues  $\mathcal{N}_{k,p}^{star} = p(k-1) + 1$ . Let  $g_{k,p}(\lambda)$  be the spectral density of  $\mathbf{S}_{k,p}$ ,

$$g_{k,p}(\lambda) : \mathbb{R} \rightarrow \mathbb{R}, \quad (3)$$

where  $\lambda$  is an eigenvalue and its frequency (degeneracy)  $g_{k,p}(\lambda)$  is its multiplicity  $M_{k,p}(\lambda)$  divided by the total number of eigenvalues  $\mathcal{N}_{k,p}^{star}$ . The probability of a star to have parameters  $k$  and  $p$  is  $\mathbb{P}(k|p)\mathbb{P}(p)$ . Specifically, we consider the ensemble of stars with fixed  $p$ , where  $k$  is distributed as in (1):

$$\mathbb{P}_\mu(k|p) = Ce^{-\mu k}, \quad \sum_{k=1}^{\infty} \mathbb{P}_\mu(k|p) = 1, \quad \sum_{p \geq 1} \mathbb{P}_\mu(p) = 1.$$

Thus, the spectral density  $g_p(\lambda)$  of the  $p$ -branch star ensemble is

$$g_p(\lambda) = \frac{\sum_{k=1}^{\infty} \mathbb{P}_\mu(k|p) M_{k,p}(\lambda)}{\sum_{k=1}^{\infty} \mathbb{P}_\mu(k|p) \mathcal{N}_{k,p}^{star}}. \quad (4)$$

We suppose that  $p \geq 3$ , since  $p = 1, 2$  corresponds to linear chains.

Below we provide numeric and analytic results for spectral densities of dendrimer ensembles. Numeric simulations allow us to make some plausible conjectures about individual graph spectra, as well as to understand generic feature of corresponding spectral densities of systems under consideration. The main steps of numeric algorithm are as follows. We calculate eigenvalues of  $\mathbf{T}_k$  or  $\mathbf{S}_{k,p}$  with corresponding multiplicities and construct a histogram. Specifically, it means that we divide the axis of eigenvalues into the intervals of length  $\Delta$  and construct a piecewise constant function  $\hat{f}_k(\lambda) : \mathbb{R} \rightarrow \mathbb{R}$ . On a segment function  $\hat{f}_k(\lambda)$  is equal to the number of eigenvalues entering this segment:

$$\hat{f}_k(\lambda) = \frac{\#\{\lambda_i \in [\lambda_{min} + l\Delta; \lambda_{min} + (l+1)\Delta]\}}{\mathcal{N}}, \quad \forall \lambda \in [\lambda_{min} + l\Delta; \lambda_{min} + (l+1)\Delta],$$

where  $\lambda_i$  is an eigenvalue, and  $l$  is an integer. Since the maximal eigenvalue is bounded (see [15]) by  $|\lambda_{\max}^{\text{tree}}| \leq 2\sqrt{p-1}$ , we can scan the support  $[-|\lambda_{\max}^{\text{tree}}|; |\lambda_{\max}^{\text{tree}}|]$  containing all eigenvalues. Finding optimal value of  $\Delta$  making the histogram most representative, is a separate technical question which is not addressed here. With such histograms for graphs (full binary trees or stars) for various values of level  $k$  we can easily reconstruct the desired spectral density by performing convolutions of the functions  $\rho_k(\lambda)$  and  $g_{k,p}(\lambda)$  with the distribution functions as it is prescribed by (2) and (4).

### III. RESULTS

#### A. Full binary trees: numerics

For full binary trees of  $k$  levels we compute spectra up to  $k = 12$ . The computational complexity for eigenvalue calculation is  $O(n^3)$ . Note that accumulating small computational errors can lead to inaccurate results. Since the maximal vertex degree of a full binary tree is  $p = 3$ , according to the inequality mentioned above, one has  $|\lambda_{\max}^{\text{tree}}| \leq 2\sqrt{2}$  for any  $k$ . In the Table Ia we provide numeric data for full binary trees main peaks multiplicities for  $k = 8, 9, 10$ . Note that diagonals in this table are relatively stable. In the Table Ib we present the main peak frequencies for  $k = 8, 9, 10$  and also for exponentially distributed ensembles with  $\mu = 0.5$  and  $\mu = 0.8$ . Note that frequencies in lines with fixed peak number are also relatively stable regardless of tree size or even whether it is an individual tree or an ensemble. Typical spectral density of a tree is depicted in the Fig. 4a and spectral density of an ensemble in the Fig. 4b. Main peaks there are enumerated.

#### B. Full binary trees: theory

##### 1. Spectral density of a single full binary tree

Following [16, 17] denote by  $\mathcal{B}_k$  a generalized Bethe tree of  $k$  levels, which is a rooted unweighted and undirected tree shown in Fig. 3. Enumerate the levels down-up by index  $j = 1, \dots, k$ . The root is located at  $j = 1$  and the number of vertices at the level  $j$  is  $n_{k-j+1}$ , all of them have equal degree  $d_{k-j+1}$ . In particular,  $d_k$  is the degree of the root,

Peak No.	$k = 8$	$k = 9$	$k = 10$
1	85	171	341
2	37	73	146
3	17	34	68
4	8	17	33
5	4	8	16

(a)

Peak No.	$\mu = 0.5$	$\mu = 0.8$	$k = 8$	$k = 9$	$k = 10$
1	0.346	0.392	0.333	0.335	0.333
2	0.146	0.152	0.145	0.143	0.143
3	0.067	0.062	0.067	0.067	0.068
4	0.032	0.029	0.031	0.033	0.032
5	0.015	0.012	0.016	0.016	0.016

(b)

Table I: (a) Individual trees: peak multiplicities for various  $k$  in enveloping series; (b) Ensemble of trees with  $\mu = 0.5$  and  $\mu = 0.8$ : peak frequencies for various  $k$  in enveloping series.

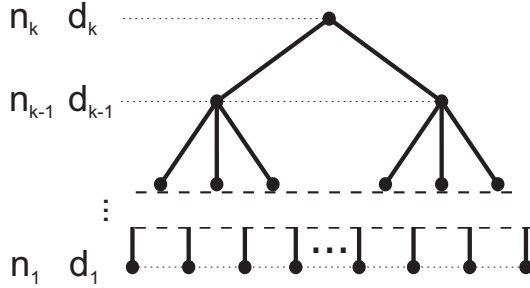


Figure 3: A generalized Bethe lattice.

$n_k = 1$  and  $n_1$  is the number of terminal vertices (“leaves”). Let  $\mathbf{A}(\mathcal{B}_k)$  be the adjacency matrix of  $\mathcal{B}_k$  and  $\sigma(\mathbf{A}(\mathcal{B}_k))$  – its spectrum. In [17] the proof of the following theorem is provided. Let us also define:  $\mathbf{A}_j(\mathbf{d}) = \mathbf{A}_j(1, d_2, \dots, d_k)$  and  $\Omega = \{j : 1 \leq j \leq k-1, n_j > n_{j+1}\}$ .

**Theorem 1.** If  $\mathbf{A}_j(\mathbf{d})$  is the  $j \times j$  leading principal submatrix of the  $k \times k$  symmetric tridiagonal matrix

$$\mathbf{A}_k(\mathbf{d}) = \begin{bmatrix} 0 & \sqrt{d_2 - 1} & & & & & \\ \sqrt{d_2 - 1} & 0 & \sqrt{d_3 - 1} & & & & \\ & \sqrt{d_3 - 1} & 0 & & & & \\ \dots & \dots & \dots & \dots & \dots & \dots & \dots \\ & & & 0 & \sqrt{d_k - 1} & & \\ & & & & \sqrt{d_k - 1} & 0 & \sqrt{d_k} \\ & & & & & \sqrt{d_k} & 0 \end{bmatrix}$$

then

- $\sigma(\mathbf{A}(\mathcal{B}_k)) = \left( \bigcup_{j \in \Omega} \sigma(\mathbf{A}_j(\mathbf{d})) \right) \cup \sigma(\mathbf{A}_k(\mathbf{d}))$ .
- The multiplicity of each eigenvalue of the matrix  $\mathbf{A}_j(\mathbf{d})$  as an eigenvalue of  $\mathbf{A}(\mathcal{B}_k)$  is  $(n_j - n_{j+1})$  for  $j \in \Omega$ , and eigenvalues of  $\mathbf{A}_k(\mathbf{d})$  as eigenvalues of  $\mathbf{A}(\mathcal{B}_k)$  are simple.

Recall that  $\mathcal{T}_k$  is a full binary tree and  $\mathbf{T}_k$  is its adjacency matrix. If the vertices are enumerated linearly through levels 1 to  $k$ , it takes the following form:

$$\mathbf{T}_k = \begin{bmatrix} 0 & 1 & 1 & 0 & 0 & 0 & 0 \\ 1 & 0 & 0 & 1 & 1 & 0 & 0 \\ 1 & 0 & 0 & 0 & 0 & 1 & 1 \\ 0 & 1 & 0 & 0 & 0 & 0 & 0 \\ 0 & 1 & 0 & 0 & 0 & 0 & 0 \\ 0 & 0 & 1 & 0 & 0 & 0 & 0 \\ 0 & 0 & 1 & 0 & 0 & 0 & 0 \end{bmatrix}$$

Here  $k = 3$ , and for other  $k$  the structure is the same. However, we do not operate this form, instead, we use the notation, introduced above.

The graph  $\mathcal{T}_k$  has  $n_{k-j+1} = 2^{j-1}$  vertices at the level  $j$ , all of degree  $d_j = 3$  except for the level  $d_1 = 1$  and the root  $d_k = 2$ . According to Theorem 1, its spectrum is the union:

$$\sigma(\mathbf{T}_k) = \bigcup_{j=1}^k \sigma(\mathbf{A}_j),$$

where  $\mathbf{A}_j$  is the following:

$$\mathbf{A}_j = \sqrt{2} \begin{bmatrix} 0 & 1 & & & & \\ 1 & 0 & 1 & & & \\ \dots & \dots & \dots & \dots & \dots & \dots \\ & & 1 & 0 & 1 & \\ & & & 1 & 0 & \\ & & & & 1 & 0 \end{bmatrix}$$

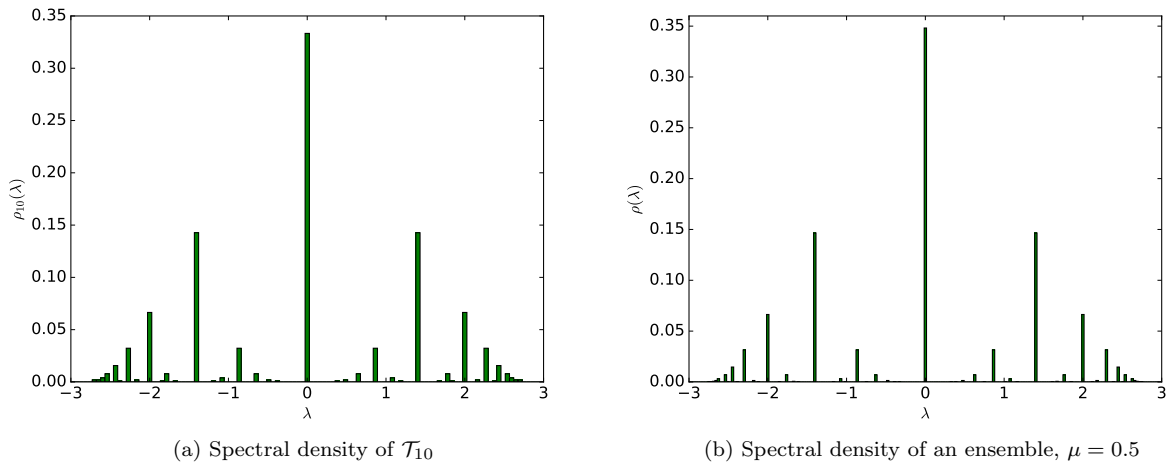


Figure 4: Eigenvalue distribution for full binary trees.

Denote  $\hat{\mathbf{A}}_j = \frac{1}{\sqrt{2}} \mathbf{A}_j$  and  $\hat{\lambda} = \frac{1}{\sqrt{2}} \lambda$ . The characteristic polynomial  $F_j = \det(\hat{\mathbf{A}}_j + \hat{\lambda}\mathbf{E})$  of the matrix  $\hat{\mathbf{A}}_j$  satisfies the following recurrence equation:

$$\begin{cases} F_{j+1} = \hat{\lambda}F_j - F_{j-1}, \\ F_0 = 1, F_1 = \hat{\lambda}. \end{cases}$$

and the corresponding characteristic equation  $\mu^2 - \mu\hat{\lambda} + 1 = 0$  has roots

$$\mu_{\pm} = \frac{\hat{\lambda} \pm \sqrt{\hat{\lambda}^2 - 4}}{2}.$$

which allows us to reconstruct the explicit form of  $F_j$ :

$$F_j = \frac{1}{\sqrt{\hat{\lambda}^2 - 4}} \mu_+^{j+1} - \frac{1}{\sqrt{\hat{\lambda}^2 - 4}} \mu_-^{j+1}. \quad (5)$$

The solution of equation  $F_j = 0$  is:

$$\hat{\lambda} = 2 \cos \frac{\pi i}{j+1}, \quad i = 1 \dots j.$$

Thus, the eigenvalues of the matrix  $\mathbf{A}_j$  are

$$\lambda = 2\sqrt{2} \cos \frac{\pi i}{j+1}, \quad i = 1 \dots j,$$

Collecting all intermediate results, we arrive at the following explicit expression for the spectrum of an individual tree  $\mathcal{T}_k$ :

$$\sigma(\mathbf{T}_k) = \bigcup_{j=1}^k \bigcup_{i=1}^j \left\{ 2\sqrt{2} \cos \frac{\pi i}{j+1} \right\}. \quad (6)$$

According to the second statement of Theorem 1, let us compute eigenvalue multiplicities. The contribution of the  $j^{\text{th}}$  principal submatrix is:

$$m_j = n_j - n_{j+1} = 2^{k-j-1} \quad (j = 1 \dots k-1), \quad m_k = 1.$$

Recall that the multiplicity of the eigenvalue  $\lambda$  is  $M_k(\lambda)$ . Then we have:

$$M_k(\lambda) = \sum_{j=1}^k m_j \mathbb{1}\{\lambda \in \sigma(\mathbf{A}_j)\}, \quad (7)$$

where  $\mathbb{1}\{A\}$  is the indicator function:

$$\mathbb{1}\{A\} = \begin{cases} 1, & \text{if } A \text{ is true} \\ 0, & \text{otherwise} \end{cases}$$

Recall that  $\lambda \in \sigma(\mathbf{A}_j)$  if there exists an integer  $i$  such that

$$\lambda = 2\sqrt{2} \cos \frac{\pi i}{j+1}$$

Supposing that  $\frac{i}{j+1}$  is irreducible, it contributes to the spectrum as an eigenvalue of every  $(j+1)^{\text{th}}$  principal submatrix:

$$2\sqrt{2} \cos \frac{\pi i}{j+1}, \quad 2\sqrt{2} \cos \frac{2\pi i}{j+1}, \quad \dots, \quad 2\sqrt{2} \cos \frac{(n-1)\pi i}{(n-1)(j+1)}, \quad 2\sqrt{2} \cos \frac{n\pi i}{n(j+1)}$$

where  $n = \left\lfloor \frac{k+1}{j+1} \right\rfloor$ . The respective multiplicities are:

$$2^{k-(j+1)}, \quad 2^{k-2(j+1)}, \quad \dots, \quad 2^{k-(n-1)(j+1)}, \quad m_n$$

where  $m_n$  depends on  $k$  and  $j$ :

$$m_n = \begin{cases} 1, & \text{if } k \equiv j \pmod{(j+1)} \\ 2^{k-n(j+1)} = 2^{k \pmod{(j+1)}}, & \text{otherwise} \end{cases}$$

Summing the geometric series, we arrive at the following expression for the multiplicity of  $\lambda = 2\sqrt{2} \cos \frac{\pi i}{j+1}$ , defined in (7):

$$M_k(\lambda) = \begin{cases} \frac{2^k + 2^j - 1}{2^{j+1} - 1}, & \text{if } k \equiv j \pmod{(j+1)} \\ \frac{2^k - 2^{k \pmod{(j+1)}}}{2^{j+1} - 1}, & \text{otherwise} \end{cases}$$

or

$$M_k(\lambda) = \frac{2^k - 2^{k \pmod{(j+1)}}}{2^{j+1} - 1} + \mathbb{1}\{k \equiv j \pmod{(j+1)}\}.$$

Recall that  $\frac{i}{j+1}$  is irreducible.

By definition, the spectral density,  $\rho_k$ , of an individual tree of level  $k$  is

$$\rho_k(\lambda) = \frac{M_k(\lambda)}{N_k^{\text{tree}}} = \frac{1}{2^k - 1} \left( \frac{2^k - 2^{k \bmod (j+1)}}{2^{j+1} - 1} + \mathbb{1}\{k \equiv j \pmod{(j+1)}\} \right). \quad (8)$$

Since the spectrum consists of  $\lambda = 2\sqrt{2} \cos \frac{\pi i}{j+1}$ , where  $i$  and  $j+1$  are coprime, we know all the eigenvalues and all their multiplicities, and hence, we can reconstruct the desired shape of the spectrum in the parametric form.

Consider now two sequences of values, defining the envelope of the spectral density. First, we compute the outer curve, which is the series of “main” peaks, or the series of maximal eigenvalues of levels from 1 to  $k$ . Specifically, the  $j^{\text{th}}$  value in this series is

$$\lambda_j^{\text{out}} = 2\sqrt{2} \cos \frac{\pi}{j+1}, \quad j = 1, \dots, k. \quad (9)$$

Similarly we can reconstruct the inner curve, which is the enveloping curve for the series of peaks descending from the second main peak to zero. The corresponding series of eigenvalues is as follows:

$$\lambda_i^{\text{in}} = 2\sqrt{2} \cos \frac{\pi j}{2j+1} = 2\sqrt{2} \sin \frac{\pi}{2(2j+1)}, \quad j = 1, \dots, \left\lfloor \frac{k}{2} \right\rfloor. \quad (10)$$

The two equations, (9) and (10), define the parametric form of  $\rho(\lambda)$  encoded in two functions,  $\rho_k$  and  $\lambda_k$ . For  $k \gg 1$  and  $i \gg 1$  we use the Taylor expansion of cos-function

$$\lambda = 2\sqrt{2} \cos \frac{\pi}{i+1} = 2\sqrt{2} \left( 1 - \frac{\pi^2}{2(i+1)^2} \right) + o\left(\frac{1}{(i+1)^2}\right) \quad (11)$$

Inverting (11), we get

$$i+1 = \frac{\sqrt[4]{2}\pi}{\sqrt{2\sqrt{2}-\lambda}} + o\left(\frac{1}{(i+1)^2}\right) \quad (12)$$

Substituting (12) into (8), we obtain the asymptotic expression of the tail of the outer enveloping curve,  $\rho(\lambda)$ , near the spectrum edge, i.e. at  $|\lambda| \rightarrow \lambda_{\max}$ :

$$\rho_k(\lambda) = \exp\left(-\frac{\sqrt[4]{2}\pi \ln 2}{\sqrt{2\sqrt{2}-|\lambda|}}\right) + O(1) \sim \exp\left(-\frac{A}{\sqrt{\lambda_{\max}-|\lambda|}}\right), \quad A = \sqrt[4]{2}\pi \ln 2. \quad (13)$$

For the inner part of the spectrum, at  $\lambda \rightarrow 0$ , we use the Taylor expansion of the sin-function at  $i \gg 1$ :

$$\lambda = 2\sqrt{2} \sin \frac{\pi}{2(i+1)} = \frac{\pi}{\sqrt{2}(2i+1)} + o\left(\frac{1}{i+1}\right); \quad (14)$$

Inverting this expression and substituting into (8), we arrive at the following asymptotics of the enveloping curve of the inner part of the spectral density (at  $\lambda \rightarrow 0$ ):

$$\rho(\lambda) \sim \exp\left(-\frac{\sqrt{2}\pi \ln 2}{|\lambda|}\right) = \exp\left(-\frac{B}{|\lambda|}\right), \quad B = \sqrt{2}\pi \ln 2. \quad (15)$$

## 2. Spectral density of full binary tree ensembles

The spectrum of a binary tree ensemble  $\sigma^{\text{ensemble}}$  reads

$$\sigma^{\text{ensemble}} = \bigcup_{k=1}^{\infty} \sigma(\mathbf{T}_k) = \bigcup_{k=1}^{\infty} \bigcup_{j=1}^k \left\{ 2\sqrt{2} \cos \frac{\pi j}{k+1} \right\}.$$

Compare to (6), note that  $k \rightarrow \infty$ .

Recall that level  $k$  is distributed exponentially,  $\mathbb{P}_\mu(k) = (e^\mu - 1)e^{-\mu k}$ . The spectral density  $\rho(\lambda)$  of the ensemble is the following quotient:

$$\rho(\lambda) = \frac{\mathbb{E}_\mu M_k(\lambda)}{\mathbb{E}_\mu N_k} = \frac{\sum_{k=1}^{\infty} M_k(\lambda) e^{-\mu k}}{\sum_{k=1}^{\infty} (2^k - 1) e^{-\mu k}}$$

Note that both series do not always converge. Substituting here the expression for multiplicities, we get:

$$\rho\left(2\sqrt{2} \cos \frac{\pi i}{j+1}\right) = \frac{\frac{1}{2^{j+1} - 1} \sum_{k=j+1}^{\infty} (2^k - 2^{k \bmod (j+1)}) e^{-\mu k} + \sum_{k=j}^{\infty} e^{-\mu k} \mathbb{1}\{k \equiv j \bmod (j+1)\}}{\sum_{k=1}^{\infty} (2^k - 1) e^{-\mu k}}$$

For  $\mu > \ln 2$  all the series converge. Computing the corresponding geometric sums, we obtain

$$\rho\left(2\sqrt{2} \cos \frac{\pi i}{j+1}\right) = \frac{(e^\mu - 1)^2}{e^{\mu(j+1)} - 1} \quad (16)$$

For  $\mu < \ln 2$  the sums diverge, however the limit of their partial sums quotient exists, does not depend on  $\mu$  and is equal to

$$\rho\left(2\sqrt{2} \cos \frac{\pi i}{j+1}\right) = \frac{1}{2^{j+1} - 1} \quad (17)$$

Also note that expression (17) is the limit of (16) as  $\mu \rightarrow \ln 2$ .

Similarly to an individual tree, substituting (12) and (14) into (16), in both cases the tails have the following asymptotic expressions

$$\rho(\lambda) \sim \begin{cases} (e^\mu - 1)^2 \exp\left(-\frac{D}{\sqrt{\lambda_{max} - |\lambda|}}\right) & \text{for } |\lambda| \rightarrow \lambda_{max} \\ (e^\mu - 1)^2 \exp\left(-\frac{E}{|\lambda|}\right) & \text{for } |\lambda| \rightarrow 0 \end{cases}$$

where  $D = \sqrt[4]{2\pi\mu}$  and  $E = \sqrt{2\pi\mu}$ . Substituting (12) and (14) into (17), we get expressions qualitatively coinciding with (13) and (15).

We have evaluated the spectrum of a single full binary tree and the spectrum of the exponentially weighted ensemble of full binary trees computing explicitly all multiplicities/frequencies. Performed numeric computations match analytic results with high accuracy. Found nonanalytic expression of  $\rho\lambda$  at the edge of the spectrum, known as a “Lifshitz tail” [18] is typical for Anderson localization in disordered one-dimensional systems like, for example, the one-dimensional Schrödinger-like discrete operators with strong diagonal disorder. Note, however, two interesting peculiarities of considered systems: i) even a single large tree has a Lifshitz tail; ii) the spectral density of the exponentially weighted ensemble of full binary trees has the same asymptotic behavior at the edge of the spectrum, as the one of the system of exponentially weighted linear chains.

### C. Star graphs: numerics

We begin the analysis of star-like graphs by computing numerically their spectra with different parameters  $k$  and  $p$  (see Fig. 2b). In particular, we consider  $k = 1, \dots, 500$  and  $p = 3, \dots, 10$ . The spectrum of individual star graphs depends on  $k$  and  $p$  and always consists of two separate series:  $k - 1$  eigenvalues of multiplicity  $p - 1$  and  $k$  eigenvalues of multiplicity 1, see Fig. 5.

Unlike the case of full binary trees, the spectrum of ensemble of star graphs with exponential distribution in sizes, is essentially different with respect to the one of an individual star graph. Even more, the structure of the spectral density in the ensemble essentially depends on  $\mu$  as shown in Fig. 7.

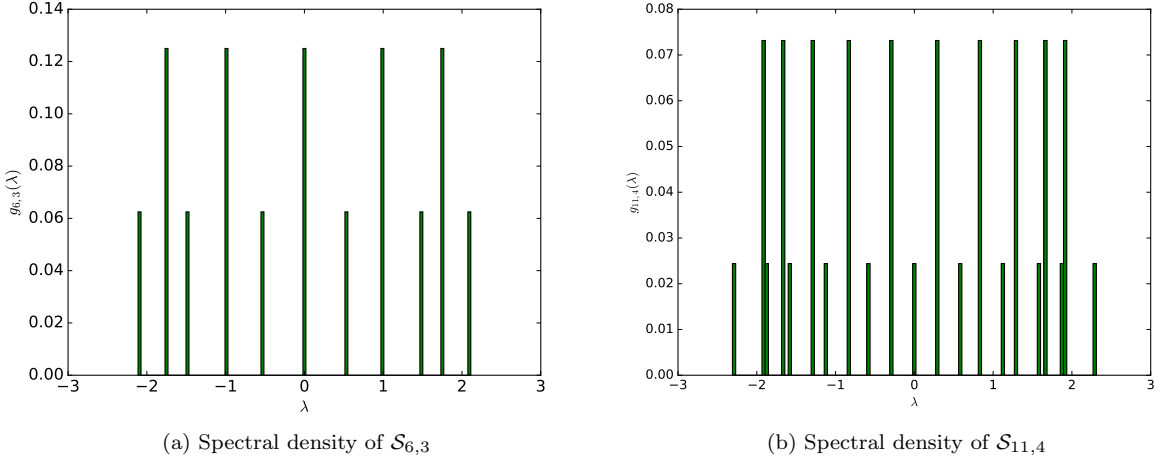


Figure 5: Eigenvalue distribution for stars.

#### D. Star graphs: theory

##### 1. Spectrum of a single star graph

For a star graph  $S_{k,p}$  of  $p$  branches and  $k$  levels, shown in Fig. 2b, according to Theorem 1 [17], the spectrum is the set of eigenvalues of  $j \times j$  principal submatrices ( $j = 1 \dots k$ ).

$$\mathbf{A}_k(S_{k,p}) = \begin{bmatrix} 0 & 1 & & & \\ 1 & 0 & 1 & & \\ & \ddots & \ddots & \ddots & \\ & & 1 & 0 & \sqrt{p} \\ & & & \sqrt{p} & 0 \end{bmatrix} \quad (18)$$

Before computing these eigenvalues, compute the corresponding multiplicities. According to Theorem 1, the contribution  $m_j$  of  $\mathbf{A}_j$  is

$$m_j = n_j - n_{j+1}, \quad j = 1 \dots k-1; \quad m_k = 1.$$

Note that for star graphs one has  $n_j = p$  for  $j = 1, \dots, k-1$ , and  $n_k = 1$ . Hence,  $m_j = 0$  for  $j = 1, \dots, k-2$ , and we only need to compute the spectra of  $\mathbf{A}_{k-1}$  (whose eigenvalues have multiplicity  $p-1$ ) and  $\mathbf{A}_k$  (whose eigenvalues are simple). Divide the spectrum of star into two parts: linear chain contribution  $\sigma_k^{lin}$  as the spectrum of  $\mathbf{A}_{k-1}$ , and center contribution  $\sigma_{k,p}^c$  as the spectrum of  $\mathbf{A}_k$ .

The roots of  $F_{k-1}$ , derived in (5), define the spectrum  $\sigma_k^{lin}$ :

$$\sigma_k^{lin} = \bigcup_{j=1}^{k-1} \left\{ 2 \cos \frac{\pi j}{k} \right\}$$

Applying the Laplace formula to the last row two times of matrix  $\mathbf{A}_k$ , we get:

$$G_k = \det \mathbf{A}_k = \lambda F_{k-1} - p F_{k-2} = \frac{p\mu_+ - \lambda}{\sqrt{\lambda^2 - 4}} \mu_-^k - \frac{p\mu_- - \lambda}{\sqrt{\lambda^2 - 4}} \mu_+^k$$

where

$$\mu_{\pm} = \frac{\lambda \pm \sqrt{\lambda^2 - 4}}{2}$$

The equation  $G_k = 0$  is equivalent to the following complex-valued transcendental equation:

$$\tan k\varphi = \frac{p}{p-2} \tan \varphi, \quad (19)$$

where we have introduced  $\varphi$  as follows:

$$\tan \varphi = \frac{\sqrt{4-\lambda^2}}{\lambda}, \quad (\lambda = 2 \cos \varphi). \quad (20)$$

The set of roots is  $\sigma_{n,p}^c$ , as introduced above. This set is always unique, except for the roots of type  $\lambda = 2 \cos \frac{\pi i}{j}$ , where  $i$  and  $j$  are coprime, or in other words, for any  $n \neq l$ :

$$(\sigma_{n,p}^c \cap \sigma_{l,p}^c) \setminus \sigma^{lin} = \emptyset$$

And also for any  $n$

$$\sigma_{n,p}^c \cap \sigma_n^{lin} = \emptyset$$

As  $\lambda_k^{max}$  is always the eigenvalue of  $\mathbf{A}_k$ , it always belongs to  $\sigma_{k,p}^c$ . Analysis shows that  $\lambda_k^{max}$  lies in the interval  $(\sqrt{p}, \frac{p}{\sqrt{p-1}})$  and is the only root in this interval for  $k \geq 2$ . Despite (19) cannot be solved exactly, a transparent analysis of its solution is available.

Here is the brief explanation how we localize the maximal root,  $\lambda_k^{max}$  for various  $p$  and  $k$ . Computing  $G_k$  for small  $k$ , we get ( $p \geq 3$ )

$$\begin{aligned} G_2 &= \lambda^2 - p & \Rightarrow \lambda_2^{max} &= \sqrt{p}, \\ G_3 &= \lambda(\lambda^2 - (p+1)) & \Rightarrow \lambda_3^{max} &= \sqrt{p+1} \\ &&& \dots \end{aligned}$$

For  $\lambda \geq 2$  Eq. (20) is transformed into the real-valued equation:

$$\tanh \varphi = \frac{\sqrt{\lambda^2 - 4}}{\lambda} \quad (\lambda = 2 \cosh \varphi)$$

For  $\varphi > 0$  Eq. (19) has either no roots, or the only root since the functions  $y_k(\varphi) = \tanh k\varphi$  and  $z(\varphi) = \frac{p}{p-2} \tanh \varphi$  are both monotone and concave, see Fig. 6. Thus, for  $k > \frac{p}{p-2}$  there is always a single solution. Note that  $p \geq 3$ , so  $\frac{p}{p-2} \leq 3$ . Also note that if  $k > l$ ,  $y_k > y_l$  for any  $\varphi > 0$ . As a result,  $\lambda_k^{max}$  is strictly monotonic and  $\lambda_2^{max} = \sqrt{p}$  is the minimal value in this series. For any  $k$  the function  $y_k(\varphi) < 1$ , thus the upper bound for the solution is:

$$z(\varphi) = 1 \Rightarrow \lambda = \frac{p}{\sqrt{p-1}}$$

As stated above, the spectrum of the star graph is the union of two spectra:

$$\sigma(\mathbf{S}_{k,p}) = \sigma_k^{lin} \cup \sigma_{k,p}^c = \bigcup_{j=1}^{k-1} \left\{ 2 \cos \frac{\pi j}{k} \right\} \cup \sigma_{k,p}^c.$$

Spectral density of an individual star graph, as defined in (3) is

$$g_{k,p}(\lambda) = \frac{M_k(\lambda)}{p(k-1)+1} = \begin{cases} \frac{p-1}{p(k-1)+1}, & \text{if } \lambda \in \sigma_k^{lin}, \\ \frac{1}{p(k-1)+1}, & \text{if } \lambda \in \sigma_{k,p}^c \end{cases}$$

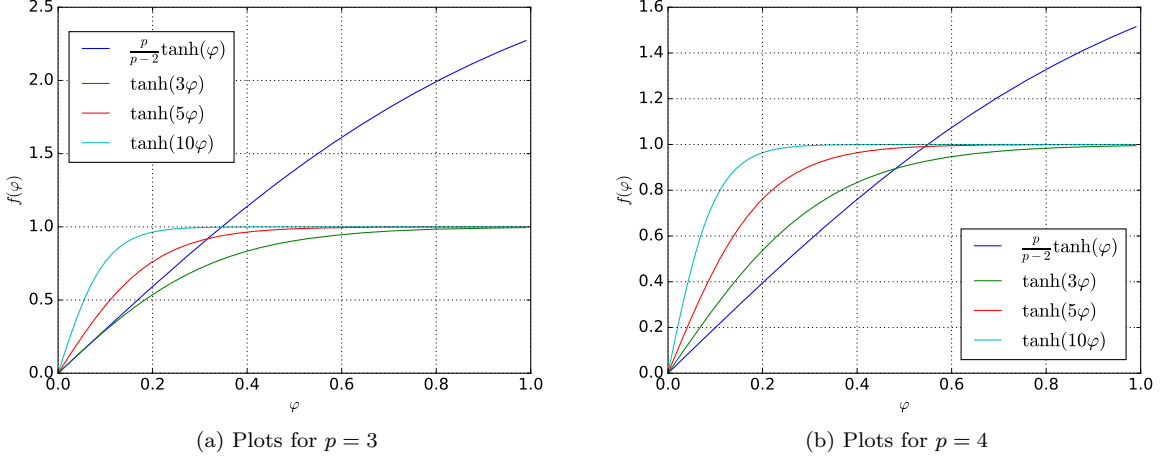


Figure 6: Illustration of graphic solution of (19).

## 2. Spectral density of ensemble of star graphs

The spectral density of a star graph ensemble is defined by the following equation:

$$\sigma_p^{ens} = \sigma^{lin} \cup \sigma_p^c,$$

where

$$\sigma^{lin} = \bigcup_{k=2}^{\infty} \sigma_k^{lin} = \bigcup_{k=2}^{\infty} \bigcup_{j=1}^{k-1} \left\{ 2 \cos \frac{\pi j}{k} \right\}, \quad \sigma_p^c = \bigcup_{k=1}^{\infty} \sigma_{k,p}^c.$$

In this case, the corresponding spectral density is the sum of contributions coming from “arms” and the “root”,

$$g_p(\lambda) = g_p^{lin}(\lambda) + g_p^c(\lambda)$$

Any  $\lambda \in \sigma^{lin}$  can be written in the form  $\lambda = 2 \cos \frac{\pi i}{j}$ , where  $i$  and  $j \in \mathbb{N}$  and are coprime. Such  $\lambda$  belongs to  $\sigma_{t,j}^{lin}$  for any  $t \in \mathbb{N}$  with the multiplicity  $p-1$ . Then spectral density,  $g_p^{lin}(\lambda)$  reads:

$$g_p^{lin}(\lambda) = \frac{\sum_{k=1}^{\infty} e^{-\mu k} (p-1) \mathbb{1}\{\lambda \in \sigma_k^{lin}\}}{\sum_{k=1}^{\infty} (p(k-1)+1) e^{-\mu k}} = \frac{(p-1) \sum_{k=1}^{\infty} e^{-\mu j k}}{\sum_{k=1}^{\infty} (p(k-1)+1) e^{-\mu k}} \quad (21)$$

Both series, in the nominator and in the denominator of (21), converge for any  $\mu > 0$ . Evaluating these series, we get:

$$g_p^{lin}(\lambda) = \frac{(p-1)(e^{\mu} - 1)^2}{(e^{\mu j} - 1)(e^{\mu} + p - 1)}$$

The function  $g_p^{lin}(\lambda)$  is the rescaled spectral density of the linear chain ensemble, derived in [4]:

$$g_p^{lin}(\lambda) = \frac{(p-1)e^{-\mu}}{1 + (p-1)e^{-\mu}} \rho_{lin}(\lambda) = \frac{(p-1)e^{-\mu}}{1 + (p-1)e^{-\mu}} \lim_{\substack{N \rightarrow \infty \\ \varepsilon \rightarrow 0}} \frac{\varepsilon}{\pi N} \sum_{n=1}^N \mu^n \sum_{k=1}^n \frac{1}{(\lambda - 2 \cos \frac{\pi k}{n+1})^2 + \varepsilon^2} \quad (22)$$

Hence,  $g_p^{lin}(\lambda)$  shares all the properties of  $\rho_{lin}(\lambda)$ . For some unique eigenvalue  $\lambda$  from  $\sigma_p^c$ , such that  $\lambda \in \sigma_{k,p}^c$  one has:

$$g_p^c(\lambda) = \frac{e^{-\mu k}}{\sum_{k=1}^{\infty} (p(k-1)+1) e^{-\mu k}} = \frac{e^{-\mu k} (e^{\mu} - 1)^2}{e^{\mu} + p - 1}$$

Most of the values from  $\sigma_p^c$  are unique as they generally do not satisfy  $\lambda = 2 \cos \frac{\pi i}{j}$ . We should also point out that  $\lambda = 0$  belongs to  $\sigma_{k,p}^c$  for any odd  $k$  and to  $\sigma_k^{lin}$  for any even  $k$ :

$$g_p^c(0) = \frac{\sum_{k=1}^{\infty} e^{-\mu(2k-1)}}{\sum_{k=1}^{\infty} (p(k-1)+1)e^{-\mu k}} = \frac{(e^\mu - 1)^2}{(e^{2\mu} - 1)(1 + (p-1)e^{-\mu})}$$

and

$$g_p^{lin}(0) = \frac{(p-1)(e^\mu - 1)^2}{(e^{2\mu} - 1)(e^\mu + p - 1)}$$

Thus, we get that frequency (degeneracy) of the central peak does not depend on  $p$ :

$$g_p(0) = g_p^{lin}(0) + g_p^c(0) = \frac{e^\mu - 1}{e^\mu + 1}$$

This result is perfectly consistent with numeric simulations. Even more, (22) shows that the connection we assumed, does exist – see Fig. 7.

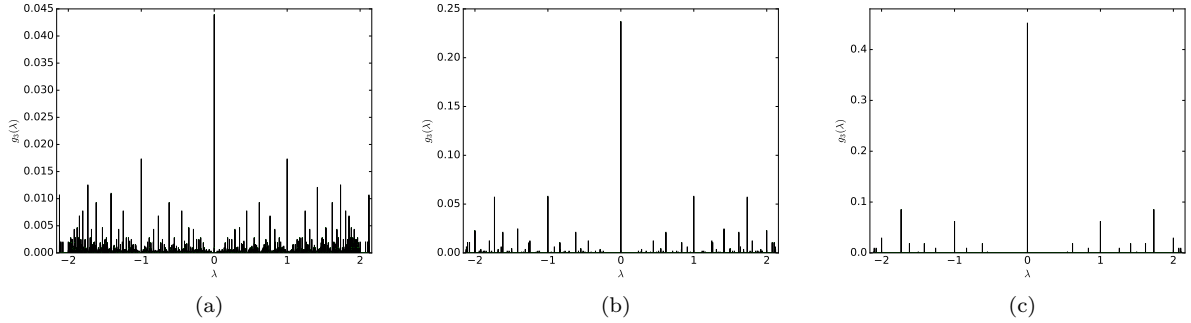


Figure 7: Eigenvalue distribution of star-like graphs with root branching  $p = 3$  in exponential ensembles with various  $\mu$ : (a)  $\mu = 0.1$ , (b)  $\mu = 0.5$ , (c)  $\mu = 1.0$ .

#### IV. CONCLUSION

In this work we have investigated the spectral statistics of exponentially weighted ensembles of full binary trees and  $p$ -branching star graphs. We have shown that corresponding spectral densities demonstrate peculiar ultrametric structure, typical for sparse graphs.

Both models, presented in the work, the fully branching 3-valent trees and the star-like graphs, have interesting peculiarities which are worth mentioning:

- The spectral density of a *single* tree already has the ultrametric behavior, which is changed only quantitatively when we pass from a single tree to the ensemble of trees exponentially distributed in their sizes.
- The spectral density of the exponential ensemble of trees looks very similar to the one of linear chains, sharing the same asymptotic behavior of tails of the distribution,  $\sim e^{-c/\sqrt{\lambda_{max}-\lambda}}$ , where for  $p$ -branching trees one has  $\lambda_{max} = 2\sqrt{p-1}$  (i.e. for linear chains  $p = 2$  and  $\lambda_{max}^{lin} = 2$ , while for 3-branching trees  $p = 3$  and  $\lambda_{max}^{tree} = 2\sqrt{2}$ ).
- The spectral statistics of  $p$ -branching star-like graphs strongly depends on  $p$  (the branching of the root point) and on  $\mu$  (the parameter in the exponential distribution of graphs sizes).

The edge singularity  $\sim e^{-c/\sqrt{\lambda_{max}-\lambda}}$  at  $\lambda \rightarrow \lambda_{max}$  reproduces the corresponding Lifshitz tail of the one-dimensional Anderson localization in a random Schrödinger operator [18–20] with strong disorder:  $\rho(E) \sim e^{-1/E^{d/2}}$  where  $E = \lambda_{max} - \lambda$  and  $d = 1$ . The appearance of the edge singularity  $\rho(E) \sim e^{-1/\sqrt{E}}$  in our situation is purely geometric, it does not rely on any entropy-energy-balance consideration like optimal fluctuation [18, 19]. Moreover, we should emphasize some universality of a “Lifshitz tail”: typically, Anderson localization appears for random three-diagonal operators with the randomness on the main diagonal, while in our case there is no diagonal disorder and the edge singularity has a kind of a number theoretic signature.

In a more practical setting, our analysis is applicable to investigation of polydisperse (i.e. distributed in sizes) diluted solutions of fully branched dendrimers (tree-like polymers). We have mentioned in the Introduction that spectral properties of adjacency matrices can be easily translated to the one of Laplacian matrices defining the relaxation modes of the system. Thus, we anticipate that ultrametricity could be directly seen in the measurements of the response of the diluted solution of noninteracting dendrimers of various sizes and topologies, on external excitations.

### Acknowledgments

The authors are very grateful to M. Tamm and K. Polovnikov for numerous discussions and valuable comments. SN acknowledges the partial support of the IRSES grant “DIONICOS” and the RFBR grant 16-02-00252a. VK and YM are supported in part by the grant of the President of Russia for young PhD MK-9662.2016.9 and by the RFBR grant 15-07-09121a. The work at LANL was carried out under the auspices of the National Nuclear Security Administration of the U.S. Department of Energy under Contract No. DE-AC52-06NA25396

---

[1] A. E. Brouwer and W. H. Haemers, *Spectra of graphs*, Springer Science & Business Media (2011)

[2] B. Mohar, *Some applications of Laplace eigenvalues of graphs*, (Springer: 1997)

[3] F. R. Chung, *Spectral graph theory*, (American Math. Soc.: 1997)

[4] V. Avetisov, P. Krapivsky, and S. Nechaev, Native ultrametricity of sparse random ensembles, *J. Phys. A: Math. Theor.*, **49** 035101 (2015)

[5] M. Planat,  $1/f$  Frequency Noise in a Communication Receiver and the Riemann Hypothesis, [the series Lecture Notes in Physics], *Noise, Oscillators and Algebraic Randomness*, **550** 265 (2000)

[6] C. Kamp and K. Christensen, Spectral analysis of protein-protein interactions in *Drosophila melanogaster*, *Phys. Rev. E*, **71** 041911 (2005)

[7] J. Mairal, F. Bach, and J. Ponce, Sparse Modeling for Image and Vision Processing. Foundations and Trends in Computer Graphics and Vision, **8(2-3)** 85 (2014)

[8] T. Peleg, Y. C. Eldar, and M. Elad, Exploiting statistical dependencies in sparse representations for signal recovery, *IEEE Trans. Signal Processing*, **60**, 2286 (2012)

[9] E. Vanden-Eijnden and J. Weare, Rare event simulation of small noise diffusions, *Comm. Pure Appl. Math.*, **65** 1770 (2012)

[10] V. Trifonov, L. Pasqualucc, R. Dalla-Favera, and R. Rabidan, Fractal-like distributions over the rational numbers in high-throughput biological and clinical data, *Scientific Reports*, **1** 191 (2011)

[11] F. Fürstenberg, M. Dolgushev, and A. Blumen, Analytical model for the dynamics of semiflexible dendritic polymers, *J. Chem. Phys.*, **136** 154904 (2012)

[12] M. Mezard, G. Parisi, and M. Virasoro, *Spin glass theory and beyond*, (World Scientific: 1987)

[13] H. Frauenfelder, *Nature Str. Biol.*, **2** 821 (1995)

[14] P.-G. de Gennes, *Scaling concepts in polymer physics*, (Cornell Univ. Press: 1979)

[15] A. Y. Grosberg and S. K. Nechaev, From statistics of regular tree-like graphs to distribution function and gyration radius of branched polymers, *J. Phys. A: Math. Theor.*, **48** 345003 (2015)

[16] O. Rojo, R. Soto, The spectra of the adjacency matrix and Laplacian matrix for some balanced trees, *Linear algebra and its applications*, Elsevier, **403** 97 (2005)

[17] O. Rojo and M. Robbiano, An explicit formula for eigenvalues of Bethe trees and upper bounds on the largest eigenvalue of any tree, *Lin. Algebra Appl.*, **427** 138 (2007)

[18] I. M. Lifshitz, Theory of fluctuation levels in disordered systems, *Sov. Phys. JETP*, **26** 462 (1968)

[19] I. M. Lifshitz, S. A. Gredeskul, and L. A. Pastur, *Introduction to the theory of disordered systems*, (Wiley-Interscience: 1988)

[20] W. Kirsch and I. Veselic, Lifshitz Tails for a Class of Schrödinger Operators with Random Breather-Type Potential, *Lett. Math. Phys.* **94** 27 (2010)